

Excitation Induced Dephasing in Semiconductor Quantum Dots

H. C. Schneider

*Physics Department, Kaiserslautern University of Technology,
P. O. Box 3049, 67653 Kaiserslautern, Germany*

W. W. Chow

*Semiconductor Materials and Device Science Department,
Sandia National Laboratories, Albuquerque, NM 87185-0601*

S. W. Koch

Physics Department, Philipps University, Renthof 5, 35037 Marburg, Germany
(Dated: March 2, 2019)

A quantum kinetic theory is used to compute excitation induced dephasing in semiconductor quantum dots that are coupled to a continuum of states representing a quantum well or a wetting layer. Pronounced frequency dependent broadening and nonlinear resonance shifts are predicted.

PACS numbers: 78.67Hc, 71.35.Cc

Semiconductor quantum dots are widely studied, e.g. for quantum optical applications [1] [2], quantum information processing [3], or semiconductor laser systems [4] [5]. In all these optical investigations the decoherence of the material polarization plays a decisive role. The fundamental dephasing time limits all externally controllable coherent, and quantum entanglement processes and the homogeneous broadening has important consequences for laser performance.[6] [7] [8] Measurements of polarization dephasing in self-organized quantum dots have recently been reported, [9] and excitation induced dephasing processes have been observed in interface quantum dots, where they were found to be important even at low temperatures and densities. [10]

Currently missing is a consistent microscopic theory for the excitation induced dephasing in quantum dots. The traditional analysis of scattering and dephasing processes in condensed matter systems invokes Boltzmann equation like approaches involving energy conserving transitions between the relevant quasi-particle states. For quantum dot structures such treatments are likely to fail since the discrete electronic states strongly restrict the allowed scattering possibilities [11] [12]. Hence, one has to perform a quantum kinetic analysis that avoids Markovian approximations.[13]

In this letter we present such a microscopic calculation where we evaluate the resulting equations for a model representing epitaxially grown or interface quantum dots. We assume that the Coulomb interaction is the predominant interaction mechanism between carriers in the dot states and carriers populating the continuum of scattering states in the wetting layer or the quantum well. By treating the heterostructure as a coupled system of quantum dot and quantum well, our approach is capable of describing the modification of the electronic and optical properties by the Coulomb interaction between carriers in the localized and continuum states. Our results predict distinctively different excitation dependences for the contributions from dot and well states due to the subtle interplay between the interaction induced dephasing and the renormalization of the resonance energies.

Our analysis starts from the standard many-particle Hamiltonian including Coulomb interacting electrons and holes with dipole coupling to a classical electromagnetic field [14]. Since we are modelling quantum-dot and quantum-well states interacting via the Coulomb potential, the relevant Coulomb interaction energy matrix element

$$V_{rsnm} = \sum_{\vec{q} \neq 0} V_q I_{nm}(q)^* I_{rs}(q) \quad (1)$$

contains the Fourier-transformed quantum-well Coulomb potential V_q and overlap integrals

$$I_{rs}(q) = \int d^2r \phi_r^*(r) e^{-i\vec{q} \cdot \vec{r}} \phi_s(r). \quad (2)$$

Here $\phi_n(r)$ is a carrier envelope function in the plane of the quantum well, which can be localized or delocalized, describing a dot or wetting layer state, respectively. The integral is extended over the quantum well plane.

We apply the nonequilibrium Green's functions technique [15] [16] to compute the linear optical response following the general approach presented in Ref. [17], [18]. In order to illustrate the physical effects due to the interaction between carriers in quantum-dot and quantum-well states, we treat the case of one localized state (denoted by "0" for the quantum-dot ground state) that is coupled to delocalized scattering states (denoted by k for the wetting layer

or quantum-well states) for electrons and holes. All screening contributions are evaluated using only the delocalized scattering states. Typically, in realistic systems different quantum dots are sufficiently far apart that there is no coupling between dots at different positions. If we furthermore assume identical confinement potentials for electrons and holes, the dynamical variables are the polarizations of the quantum-dot, $p_0 = \langle b_0 a_0 \rangle$, and the quantum-well, $p_k = \langle b_k a_k \rangle$. For the evaluation of the probe absorption spectra, we retain all terms linear in the induced probe polarization and transform to frequency space. However, we do not employ a Markov approximation but retain energy dependent scattering rates.

In detail, the electron-hole polarization connecting the electron and hole ground states (“0”) is determined by

$$(\hbar\omega - \epsilon_0^e - \epsilon_0^h)p_0 + \hbar\Omega_{00}(1 - n_0^e - n_0^h) = iS_0(\omega) \quad (3)$$

with the scattering contribution

$$S_0(\omega) = -\Lambda_{00}p_0(\omega) + \sum_{\vec{k}'} \Lambda_{0,k'} p_{k'}(\omega). \quad (4)$$

In Eq. (3), the Rabi energy $\hbar\Omega_{00}$ and the quantum-dot single-particle energies ϵ_0^α ($\alpha = e, h$) are renormalized energies containing the many-body Hartree-Fock contributions. The carrier distribution functions are denoted by n_0^α . The Hartree-Fock contributions to $\hbar\Omega_{00}$ and ϵ_0^α are linear in the bare Coulomb potential [14], whereas the correlation (or scattering) contributions $S_0(\omega)$ are given in 2nd Born approximation.[18] Since we assume a quasi-equilibrium situation with temporally constant electron and hole populations, we can analytically evaluate the Fourier transform of the non-Markovian dynamical equation for the scattering contributions that determine the optical response to the weak probe pulse. The result for the frequency dependent diagonal part is

$$\begin{aligned} \Lambda_{00}(\omega) = \Gamma_{00} - i\Delta_{00} = & \frac{1}{A^2} \sum_{\vec{q} \neq 0, \vec{k}', \vec{k}''} \sum_{\alpha, \beta=e, h} [2W_q^2 |I_{0k'}(q)|^2 - \delta_{\alpha\beta} W_q W_{k''-k'+q} I_{0k'}(q) I_{0k''}(k''-k'+q)^*] \\ & \left[(1 - n_{k'}^\alpha) n_{k''+q}^\beta (1 - n_{k''}^\beta) + n_{k'}^\alpha (1 - n_{k''+q}^\beta) n_{k''}^\beta \right] g(\hbar\omega - \epsilon_0^{\bar{\alpha}} - \epsilon_{k'}^\alpha + \epsilon_{k''+q}^\beta - \epsilon_{k''}^\beta) \end{aligned} \quad (5)$$

and correspondingly for the off-diagonal parts $\Lambda_{0,k'}$, which can be obtained from Eq. (5) by pulling the k' sum out, and making the replacements $n_{k'}^\alpha \rightarrow n_0^\alpha$ as well as $\epsilon_0^{\bar{\alpha}} - \epsilon_{k'}^\alpha \rightarrow \epsilon_0^\alpha - \epsilon_{k'}^{\bar{\alpha}}$. Here, $g(\epsilon) = \lim_{\eta \rightarrow 0} \frac{i}{\epsilon + i\eta}$ with ϵ being the Hartree-Fock renormalized energies. Furthermore, Γ_{00} is the dephasing contribution, and Δ_{00} the energy renormalization by the correlation contribution that is added to the Hartree-Fock contribution. The screened potential is denoted by $W_q = V_q/\varepsilon_q$, where ε_q is the Lindhard dielectric functions computed using the quantum-well carrier distributions, and the normalization area is denoted by A .

We choose a parabolic in-plane confinement potential for the quantum dot and a quantum-well width of $w = 4$ nm, with material parameters typical of the InGaAs/GaAs system. For the scattering states, we use orthogonalized plane waves in Eq. (2). Equations (3)–(5) couple to the microscopic quantum-well polarizations p_k , whose equations of motion are similar to those used in Markovian quantum-well calculations.[18],[19] In deriving the equations of motion for the p_k , we ignore the influence of the quantum dots on the quantum-well. Hence, we can formally obtain the equations for p_k from Eqs. (3)–(5) by replacing $0 \rightarrow k$, and $I_{0k'}(q) \rightarrow I_{kk'}(q) = \delta(k - k' + q)$.

To compute the probe absorption $\alpha(\omega)$ and refractive index $\delta n(\omega)$ spectra for the quantum-dot system, we sum the contributions from localized and delocalized states to the optical polarization according to $P(\omega) = N_{\text{dot}}\mu_{00}p_0(\omega) + \frac{1}{A} \sum_{\vec{k}} \mu_k p_k(\omega)$, where μ_{00} and μ_k are the quantum-dot and quantum-well dipole matrix elements, respectively. We then calculate $(\omega/c)\delta n(\omega) + i\alpha(\omega) = \omega/(\varepsilon_0 n_{\text{bg}} c w)P(\omega)/E(\omega)$. Here, N_{dot} is the sheet density of the quantum dots in the well, ε_0 and c are the permittivity and speed of light in vacuum, w is the quantum-well width, and n_{bg} is the background (non-resonant) refractive index. For weak probe fields we assume quasi-equilibrium between the quantum-dot and quantum-well states, as experimentally verified for electrically injected quantum-dot systems above 100K. [20] Therefore, we use quasi-equilibrium Fermi-Dirac functions $n_0^\alpha = f_0^\alpha(\mu_\alpha, T)$ and $n_k^\alpha = f_k^\alpha(\mu_\alpha, T)$, $\alpha = e, h$, where T is the temperature, and the chemical potentials μ_α are determined by the mean carrier densities $N_\alpha = 2N_{\text{dot}}n_0^\alpha + \frac{2}{A} \sum_{\vec{k}} n_k^\alpha$.

Figure 1 shows absorption spectra obtained by evaluating Eqs. (3)–(5) for different carrier densities under room-temperature ($T = 300$ K) quasi-equilibrium conditions. Each spectrum exhibits the quantum-dot resonance and the absorption due to the extended quantum-well states. With increasing carrier density, the bleaching of the quantum-dot resonance is accompanied by a pronounced red shift and excitation induced broadening. In contrast, the quantum-well exciton resonance exhibits only bleaching and broadening, but no energy shift. This excitation independent excitonic peak position in quantum wells is a consequence of the balancing between the single-particle (band-gap) shift and the

reduction of the excitonic binding energy due to phase space filling and screening of the Coulomb interaction. [18] In the quantum-dot case the cancellation is absent because the resonance energy is mostly determined by the electron and hole confinement in the quantum-dot potential, and the Coulomb attraction contribution is relatively small in comparison. Therefore, we mainly see the red shift resulting from the Hartree-Fock and scattering contributions. Such a red shift of the quantum-dot ground-state resonance has been observed recently in photoluminescence experiments [21].

As shown in Fig. 2, the non-Markovian scattering calculations predict a lineshape of the quantum-dot resonance (solid line) that significantly deviates from that of a Lorentzian lineshape function (dotted curve) obtained by a least-squares fit to the result of the full calculation. Towards low energies, the actual absorption decreases more rapidly than described by the Lorentzian. The opposite occurs at the high energy tail because of the increase in the dephasing rate $\Gamma_{00}(\omega)$ with frequency.

Figure 3 compares the spectra calculated with the full scattering terms (solid line) with a purely diagonal dephasing approximation (dashed line). In the case of the quantum dot, the spectrum is largely unchanged by the off-diagonal contributions except for the background absorption due to the quantum well. In contrast, the quantum-well exciton is completely washed out without the off-diagonal correlations.

Figure 4 summarizes the results for the excitation induced dephasing. Plotted is the full width at half maximum (FWHM), normalized to the bulk-exciton binding energy, versus carrier density. The main figure shows the difference between the full (solid curve) and Markovian (dashed curve) calculations. While both curves exhibit a linear dependence of spectral width on carrier density, using the Markovian approximation overestimates both the magnitude and the carrier density dependence. This unexpected result is a consequence of the frequency dependent effective dephasing rate and the excitation induced red shift of the dot resonance. The inset compares these results to the quantum-well broadening. In addition to an appreciably larger broadening, the quantum-well spectral width has a superlinear dependence on carrier density, compared to the linear dependence for the quantum dot. The difference in behavior between quantum-dot and quantum-well excitonic resonance is a consequence of the different scattering contributions, with a larger phase space contributing to the dephasing of the quantum-well exciton.

Comparison with experiment is best done in terms of the change in spectral width with carrier density, as it eliminates the background due to carrier-phonon scattering. We extracted values of 3 to 6×10^{-18} meV/cm⁻³ from single quantum-dot measurements [21], where the variation arises from dot-to-dot fluctuations and uncertainty in carrier density. This range of values compares favorably with our prediction of 2×10^{-18} meV/cm⁻³ (slope of solid curve in Fig. 4), where we used the quantum-well width of 4 nm and assumed $\epsilon_R = 4$ meV.

In conclusion, we present a non-Markovian quantum-kinetic analysis of the excitation dependent energy renormalization and broadening of quantum-dot states that are electronically coupled to a quantum-well like continuum of states. The dot resonance displays a density-dependent red shift, which is the counterpart of the band-gap shift for the quantum-well states, whereas the quantum-well excitonic resonance is stationary due to the compensation of gap shift and reduction of the exciton binding energy. The quantum-dot resonance shows a pronounced excitation induced dephasing, but its magnitude is smaller than that of the quantum-well excitons. The usual Markov approximation leads to an appreciable overestimation of the excitation induced dephasing for quantum dots, and should therefore be avoided in calculating quantum-dot optical spectra.

We thank W. Hoyer and M. Kira, Marburg, for helpful discussions. This work was funded in part by the United States Department of Energy under contract DE-AC04-94AL85000. WWC was supported in part by the Senior Scientist Program of the Humboldt Foundation. SWK thanks the Deutsche Forschungsgemeinschaft, the Humboldt Foundation and the Max-Planck Society for support.

[1] P. Michler, A. Imamoglu, M. D. Mason, P. J. Carson, G. F. Strouse, and S. K. Buratto, *Nature* **406**, 968 (2000).
 [2] M. Bayer, T. L. Reinecke, F. Weidner, A. Larionov, A. McDonald, and A. Forchel, *Phys. Rev. Lett.* **86**, 3168 (2001).
 [3] X. Q. Li, Y. W. Wu, D. Steel, D. Gammon, T. H. Stievater, D. S. Katzer, D. Park, C. Piermarocchi, and L. J. Sham, *Science* **301**, 809 (2003).
 [4] M. Sugawara, ed., *Self-Assembled InGaAs/GaAs Quantum Dots*, vol. 60 of *Semiconductors and Semimetals* (Academic, San Diego, 1999).
 [5] D. Bimberg, M. Grundmann, and N. N. Ledentsov, *Quantum Dot Heterostructures* (Wiley, New York, 1999).
 [6] A. V. Uskov, A. P. Jauho, B. Tromborg, J. Mork, and R. Lang, *Phys. Rev. Lett.* **85**, 1516 (2000).
 [7] H. C. Schneider, W. W. Chow, and S. W. Koch, *Phys. Rev. B* **66**, 041310(R) (2002).
 [8] M. Sugawara, K. Mukai, Y. Nakata, and H. Ishikawa, *Phys. Rev. B* **61**, 7595 (2000).

- [9] P. Borri, W. Langbein, S. Schneider, U. Woggon, R. L. Sellin, D. Ouyang, and D. Bimberg, Phys. Rev. Lett. **87**, 157401 (2001).
- [10] T. Guenther, C. Lienau, T. Elsaesser, M. Glanemann, V. M. Axt, T. Kuhn, S. Eshlaghi, and A. D. Wieck, Phys. Rev. Lett. **89**, 057401 (2002).
- [11] Y. Toda, O. Moriwaki, M. Nishioka, and Y. Arakawa, Phys. Rev. Lett. **82**, 4114 (1999).
- [12] J. Urayama, T. B. Norris, J. Singh, and P. Bhattacharya, Phys. Rev. Lett. **86**, 4930 (2001).
- [13] L. Banyai, D. B. Tran Thoai, E. Reitsamer, H. Haug, D. Steinbach, M. U. Wehner, M. Wegener, T. Marschner, and W. Stolz, Phys. Rev. Lett. **75**, 2188 (1995).
- [14] H. Haug and S. W. Koch, *Quantum Theory of the Optical and Electronic Properties of Semiconductors* (World Scientific, Singapore, 1995), 3rd ed.
- [15] W. Schäfer and M. Wegener, *Semiconductor Optics and Transport Phenomena* (Springer, 2002).
- [16] H. Haug and A.-P. Jauho, *Quantum Kinetics in Transport and Optics of Semiconductors*, vol. 123 of *Springer Series in Solid-State Sciences* (Springer, Berlin, 1996).
- [17] R. Binder and S. W. Koch, Progress Quant. Electronics **19**, 307 (1995).
- [18] G. Khitrova, H. M. Gibbs, F. Jahnke, M. Kira, and S. W. Koch, Rev. Mod. Phys. **71**, 1591 (1999).
- [19] W. W. Chow and S. W. Koch, *Semiconductor-Laser Fundamentals* (Springer, Berlin, 1999).
- [20] E. Herrmann, P. M. Smowton, H. D. Summers, J. D. Thomson, and M. Hopkinson, Appl. Phys. Lett. **77**, 163 (2000).
- [21] K. Matsuda, K. Ikeda, T. Saiki, H. Saito, and K. Nishi, Appl. Phys. Lett. **83**, 2250 (2003).

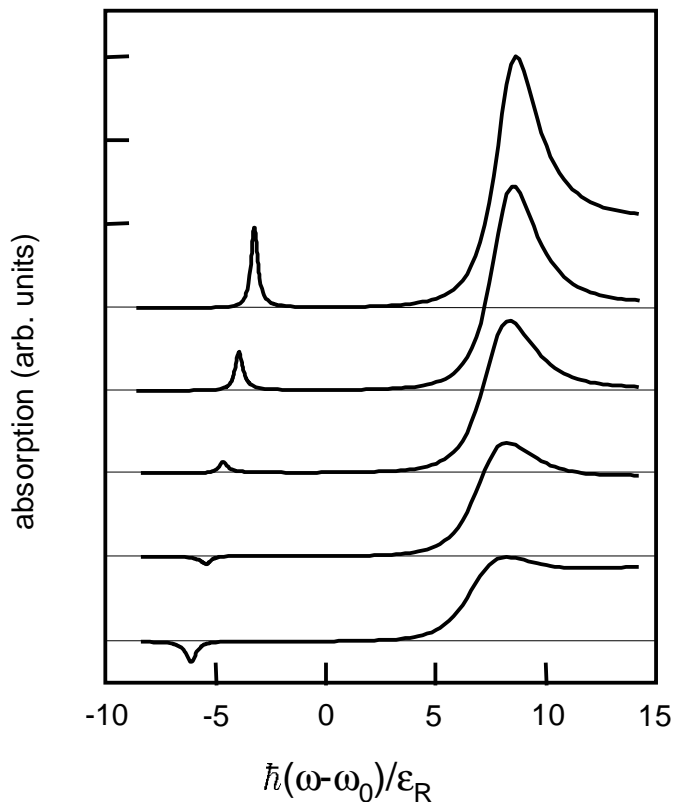


FIG. 1: Room-temperature absorption spectra for the combined quantum-dot/quantum-well system for carrier densities 2 to $4 \times 10^{11} \text{ cm}^{-2}$ in intervals of $5 \times 10^{10} \text{ cm}^{-2}$ (top to bottom, the base line of the spectra is shifted). The energy unit is the 3-dimensional exciton binding energy ϵ_R , and the zero is at the bare quantum-dot excitonic transition $\hbar\omega_0$.

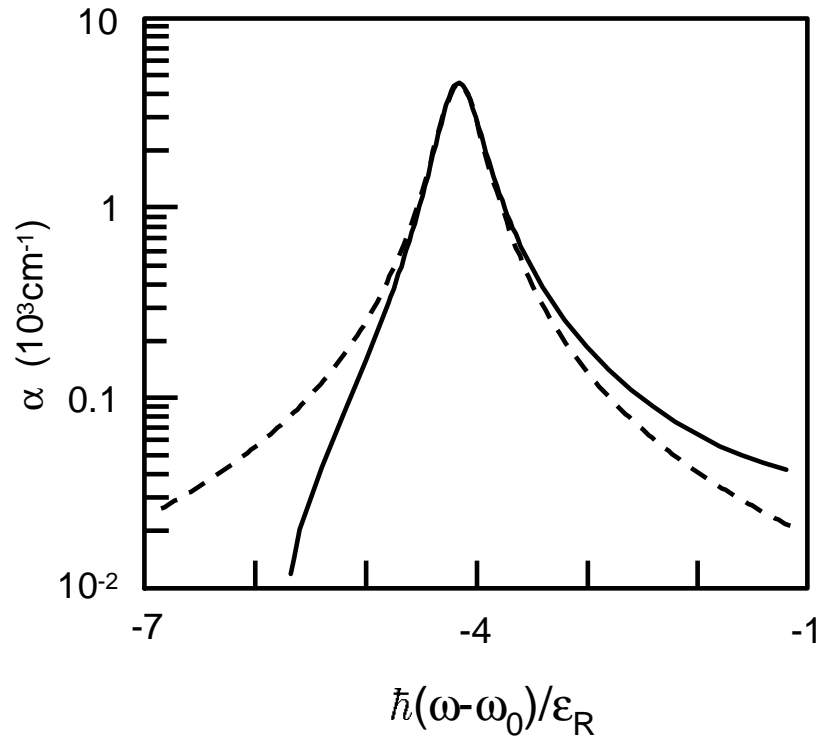


FIG. 2: Absorption spectrum around quantum-dot resonance for carrier density $2.5 \times 10^{11} \text{ cm}^{-2}$ calculated using the full non-Markovian scattering contributions (solid curve). The dotted curve is obtained from a least-squares fit with a Lorentzian.

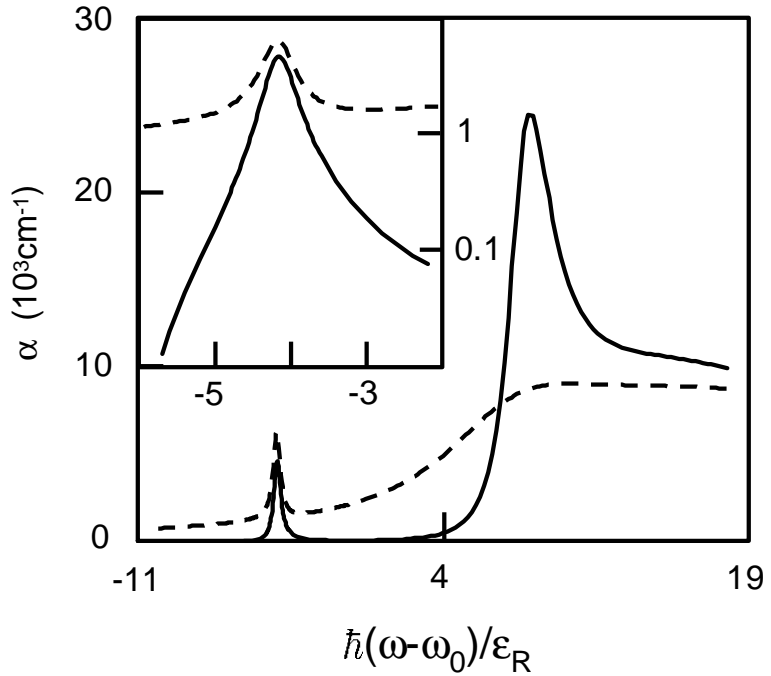


FIG. 3: Room-temperature absorption spectra for the combined quantum-dot/quantum-well system for carrier density $2.5 \times 10^{11} \text{ cm}^{-2}$ calculated using the full scattering contributions (solid line) or only the diagonal scattering contributions (dashed line). Inset: the quantum dot spectra in more detail.

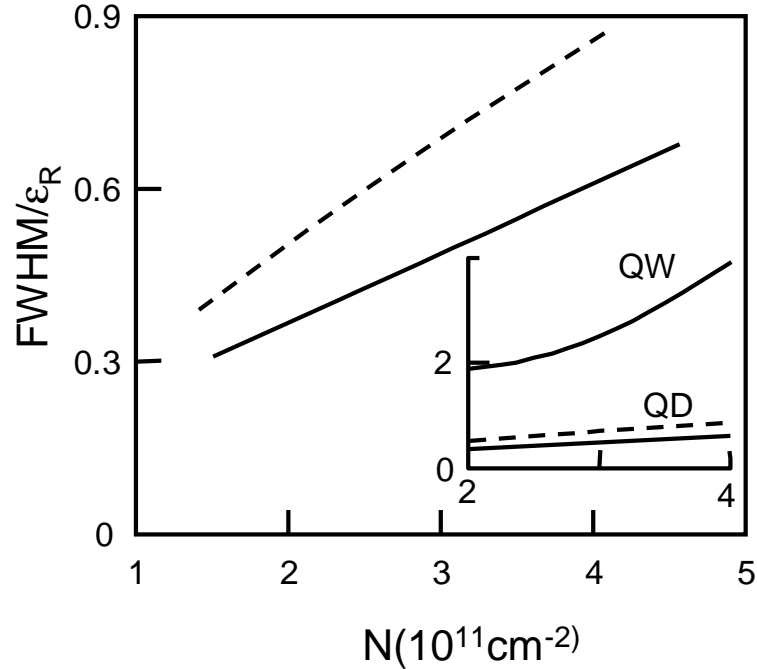


FIG. 4: Excitation dependent broadening of the quantum-dot and quantum-well resonance lines calculated using the full non-Markovian scattering contributions (solid lines) and the Markov approximation (dashed line). Inset: Comparison to excitation induced broadening of the quantum-well excitonic resonance. The energy unit is the 3-d exciton binding energy.